Separation Science and Technology
Publication details, including instructions for authors and subscription information:
http://www.informaworld.com/smpp/title~content=t713708471

Vapor Adsorption of Volatile Organic Compounds Using Organically Modified Clay

Su-Jin Park[a]; Young-Bo Kim[a]; Sang-Do Yeo[a]
[a] Department of Chemical Engineering, Kyungpook National University, Daegu, Korea

To cite this Article Park, Su-Jin , Kim, Young-Bo and Yeo, Sang-Do(2008) 'Vapor Adsorption of Volatile Organic Compounds Using Organically Modified Clay', Separation Science and Technology, 43: 5, 1174 — 1190
To link to this Article: DOI: 10.1080/01496390801910138
URL: http://dx.doi.org/10.1080/01496390801910138

Separation Science and Technology, 43: 1174–1190, 2008

ISSN 0149-6395 print/1520-5754 online
DOI: 10.1080/01496390801910138

Vapor Adsorption of Volatile Organic Compounds Using Organically Modified Clay

Su-Jin Park, Young-Bo Kim, and Sang-Do Yeo

Department of Chemical Engineering, Kyungpook National University,
Daegu, Korea

Abstract: Organically modified clay was used to adsorb volatile organic compounds from a gaseous phase. The organoclay was prepared by adsorbing hexadecyltrimethylammonium (HDTMA) on the surface of montmorillonite particles. Two volatile organic compounds (VOCs), chlorobenzene and trichloroethylene, were adsorbed to the organoclay using a fixed adsorption bed. The adsorption was carried out at various inlet concentrations of gaseous VOCs in a carrier gas (nitrogen). The adsorption behavior of VOCs was investigated using natural clay and two types of organoclays, which had different HDTMA loadings. Adsorption breakthrough curves were obtained, and the adsorption data were modeled with two adsorption isotherms. Desorption of VOCs was also conducted using pure nitrogen, and the desorption profiles were fitted with two different theoretical models. It was found that the organoclay possesses significant adsorption capacity towards VOCs and the uptake depends on the degree of HDTMA loading on clay surface.

Keywords: Organoclay, VOCs, adsorption, montmorillonite, HDTMA

INTRODUCTION

Organically modified clay (organoclay) has been used as an alternative to solid adsorbents and can be substituted for expensive solid adsorbents such as activated carbon. Natural clay particles, such as bentonite and montmorillonite,

Received 16 August 2007, Accepted 9 December 2007

Address correspondence to Sang-Do Yeo, Department of Chemical Engineering, Kyungpook National University, Daegu 702-701, Korea. Tel.: +82-53-950-5618; Fax: +82-53-950-6615; E-mail: syeo@knu.ac.kr

have a hydrophilic nature. However the clays can be modified to have organophilic characteristics by exchanging their surface ions with cationic surfactants (1, 2). The organoclays show a dramatically enhanced immobilizing and sorption power towards various environmental contaminants such as phenols, PCBs, and PAHs (3, 4). The major research interest in organoclays include the adsorption of organic compounds from liquid media such as waste water. Studies have focused on the adsorption kinetics and adsorption capacity for toxic organic materials, and the researchers have measured adsorption isotherms and equilibrium behavior between organoclays and aqueous media (5–7). However, the adsorption from gaseous phase has rarely been conducted for organoclays, which might be worth investigating in order to develop inexpensive adsorbents for the removal of air contaminants such as volatile organic compounds (VOCs).

Modification of the surface properties of natural clays is made by a simple ion exchange with organic cations. Among the many types of natural clays, montmorillonite is easily modified by exchanging its inorganic cations with quaternary ammonium cations, which may result in an increase in the inter-lamellar spacing and exposure of new adsorption sites for organic compounds (8, 9). The adsorption sites of the organoclay include both the external surface and the enlarged inter-lamellar spacing of the particles which may provide the selectivity due to the creation of a sorption zone (or phase) into which hydrophobic contaminants can be partitioned (10). The adsorption capacity and surface property of the modified clay strongly depends on the degree of surfactant loading on the clay surface. A general model of surfactant sorption on a clay surface is the formation of a monolayer or hemimicelles at the clay surface that is due to the strong ionic bonds (11). Therefore, the cationic surfactant forms a stagnant layer at the interface of the clay and the adsorbing media.

The layer of surfactant on the clay surface exhibits two roles. Firstly, the layer definitely provides the sites for adsorption of the organic compounds. Therefore the higher concentration of surfactant on the clay surface will enhance the adsorption capacity for organics. Secondly, the surfactant layer may induce a mass transfer resistance for the adsorbing species which diffuse from the liquid (or gas) phase to the clay surface. Therefore, the surfactant loading on the clay surface may control the adsorption capacity as well as the mass transfer resistance for the clay particles.

In this study, we investigated the adsorption behavior of two volatile organic compounds (chlorobenzene and trichloroethylene) on montmorillonite organoclays which were modified by hexadecyltrimethylammonium (HDTMA). Two types of organoclays that had different HDTMA loadings were used. The VOCs were adsorbed from a gaseous phase (nitrogen), and the adsorption isotherms were determined by using a dynamic response technique. The desorption behavior was also investigated by using pure nitrogen, and desorption profiles were fitted with two theoretical models. This study suggests that organoclays can be utilized as possible adsorbents for air decontamination as well as for water purification.

EXPERIMENTAL METHODS

Materials

Montmorillonite was purchased from Aldrich Chemical Co. (Lot 06016PN). Hexadecyltrimethylammonium (HDTMA, in the form of a 25 wt% solution in water) which is quaternary amine cations of the form $[(CH_3)_3NR]^+$ was also purchased from Aldrich Chemical Co. (Lot 0526JN). Chlorobenzene (99.5%) and trichloroethylene (99.5%) were obtained from Junsei Chemical Co. All the chemicals were used as received.

Clay Modification

The purchased montmorillonite clay was purified by repeated washing and digestion steps using distilled water and 35% H_2O_2 solutions. The washing process removed impurities and clay organics from the base montmorillonite particles. Scanning electron microscopy showed that the average particle size of washed montmorillonite particle was ca. 20 μm. The cation- exchange capacity (CEC) of the clay sample was measured using calcium acetate ($Ca(CH_3COO)_2$) solutions. The CEC of washed clay was 50.4 meq/100 g-clay that corresponded to 161 mg HDTMA/g-clay.

The washed clay was organically modified by HDTMA. In this study, two types of organoclays that had different HDTMA loadings were prepared. First, a 5000 ppm HDTMA solution in distilled water was prepared. Next, 30 g of washed clay was added to 1000 ml of the HDTMA solution. The solution was agitated at 300 rpm for 24 hrs in order to allow the sorption of HDTMA onto the clay surface. The clay was separated from the solution by filtering and it was dried in an oven at 60°C for 24 hrs. The HDTMA loading of this organoclay was measured by a total organic carbon analyzer (TOC, TOC-5000 Shmadsu), and the loading was found to be 152 mg HDTMA/g-clay. This amount of HDTMA loading was roughly close to 100% (actually 94.4%) of the CEC of washed clay (161 mg HDTMA/g-clay). For convenience, therefore, this clay sample was named as organoclay CEC 100. In order to prepare the other type of organoclay, a 2500 ppm HDTMA solution was prepared. The HDTMA concentration of this solution was half of the concentration of the previous solution. Next, 30 g of washed clay was added to 1000 ml of the solution and the same procedure was repeated. The clay sample prepared from this procedure was named as organoclay CEC 50 because the HDTMA loading should have been reduced by half compared to organoclay CEC 100. In this study, three clay samples (washed clay, organoclay CEC 50, and organoclay CEC 100) were used in the adsorption experiments. Physical properties of the used clays are given in Table 1.

Table 1. Properties of the clays used in this study

Clay type	Surface area (m^2/g)	Pore volume (cc/g)	Pore size (Å)
Washed	150.1	0.175	38.4
CEC 50	55.8	0.107	38.2
CEC 100	21.9	0.083	38.2

Adsorption and Desorption Experiments

Two VOCs (chlorobenzene (CB) and trichloroethylene (TCE)) were adsorbed on washed clay, organoclay CEC 50, and organoclay CEC 100, respectively. Properties of the investigated VOCs are given in Table 2. Nitrogen was used as the gas-phase carrier for the VOC adsorption, and also used to desorb VOCs from clays.

Figure 1 shows the experimental apparatus used for adsorption and desorption of VOCs. The unit consists of three parts: a VOC saturator, an adsorption bed, and a gas analyzer. For adsorption experiments, the adsorption bed (7.75 mm ID, 9.5 mm OD, 310.0 mm length) was loaded with 14.5 g of clay. Next, nitrogen, whose flow rate was controlled by the mass flow controller M1, was saturated with a VOC by bubbling it through the saturator S1. Before the VOC-saturated nitrogen was introduced into the adsorption bed, the flow stream was mixed with pure nitrogen whose flow rate was controlled by the mass flow controller M2. In this way, the inlet concentration of the gas stream was adjusted as desired. During the above procedure for adjusting the inlet concentration, the gas stream passed through a bypass line to analyze the inlet concentration by a gas chromatograph. To start the adsorption, the stream was switched from the bypass to the adsorption bed, which generated the positive step change of inlet concentration. The effluent stream from the adsorption bed was analyzed using an online sampling valve and a gas chromatograph equipped with a DB-1 capillary column and a FID. The adsorption experiment was completed when the effluent concentration became close to the inlet value.

After the adsorption was finished, the desorption experiment was conducted by flowing pure nitrogen through the VOC-saturated adsorption

Table 2. Physical properties of the investigated volatile organic compounds

Property	Chlorobenzene (C_6H_5Cl)	Trichloroethylene (C_2HCl_3)
Molecular weight (g/mol)	112.5	131.4
Normal boiling point (°C)	132.0	86.9
Critical temperature (°C)	359.2	271.1
Critical pressure (bar)	44.6	49.5
Vapor pressure (25°C, kPa)	1.58	9.87

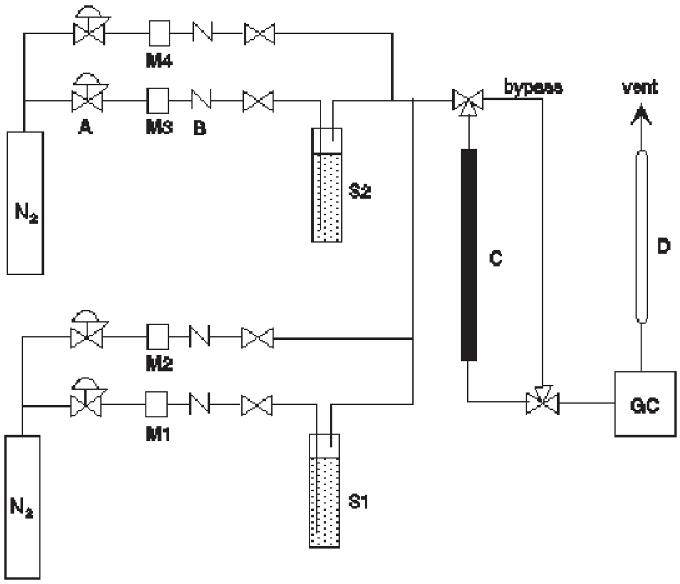

Figure 1. Experimental apparatus for adsorption and desorption of volatile organic compounds. (A) gas regulator, (B) check valve, (C) adsorption bed, (D) soap bubble meter, (M1-M4) mass flow controller, (S1-S2) VOC saturator.

bed. The concentration of VOC in the effluent stream was analyzed, and the experiment was continued until the VOC concentration in the effluent stream reached the detection limit of the gas chromatograph. The flow rate of the nitrogen stream was measured by a soap bubble meter. The nitrogen flow rate was maintained at 1.2 ml/s for both the adsorption and desorption experiments. All experiments were conducted at room temperature which is 23°C.

RESULTS AND DISCUSSION

Dynamic Response Technique

A dynamic response technique enables us to determine the amount of adsorption of VOCs based on the adsorption breakthrough curves (12). In this technique, the concentration of a VOC in the gas phase gives a positive step change at the entrance of the adsorption bed, and the responding effluent concentration is monitored as a function of time at the exit of the bed. Based on the mass balance, the resulting breakthrough curve is used to obtain the amount of VOC adsorbed on the bed. Let m_i and m_e be the masses of a VOC entering and exiting the bed, respectively, then the mass of adsorbed m_{ad} becomes equal to $m_i - m_e$. Based on this principle, the mass of adsorption in time t is calculated using the inlet concentration C_i, the effluent concentration C_e, the volume flow rate of gas phase V, and the molecular weight of an adsorbing component M as follows.

$$m_{ad} = MVC_i\left[\int_0^t (1 - C_e/C_i)dt\right] \tag{1}$$

Eq. (1) enables the calculation of the mass of adsorption based on the adsorption breakthrough curves that are obtained at various inlet concentrations. This equation also allows us to determine the amount of desorption using the desorption profiles obtained from desorption experiments.

Adsorption Breakthrough Curves

Figure 2 shows the adsorption breakthrough curves of chlorobenzene on three types of clays. The ordinate is the ratio of effluent concentration C_e to the concentration of the chlorobenzene-saturated nitrogen stream C_s. The saturated concentration of chlorobenzene in nitrogen was 15,000 ppm. The abscissa is the volume of nitrogen passed through the adsorption bed. Figure 2 is a record of effluent concentration responding to the step change of inlet concentration from zero to a particular value. Various inlet concentrations (C_i) were used in the range of $0.26–0.68C_s$ as shown in the figure legends. Figure 2 shows the effect of the HDTMA loading on organoclay on the adsorption behavior of chlorobenzene. The three plots in Fig. 2 correspond to the breakthrough curves for washed clay (a), organoclay CEC 50 (b), and organoclay CEC 100 (c), respectively. It should be noted that the ordinate and abscissa in these three plots are plotted with the same scale.

Comparison of the three plots in Fig. 2 illustrates the difference in the pattern of the breakthrough curves depending on the HDTMA loading on organoclays. The breakthrough curves for washed clay show steep slopes with the relatively delayed breakthrough points. For example, the breakthrough point for a curve obtained at inlet concentration of $0.68C_s$ occurred when 4200 ml of nitrogen was used. Then the curve sharply increased from zero to final concentration and quickly stabilized. This trend was more apparent when a higher inlet concentration was used. The shape of a breakthrough curve that has a very steep slope indicates that the adsorption of chlorobenzene on washed clay is close to an ideal adsorption system of no mass transfer resistance, no axial dispersion, and an infinitesimal width of mass transfer zone (13).

The breakthrough curves for organoclays, however, have appreciably more gentle slopes than the curves for washed clay. In addition, the slopes of curves for organoclay CEC 100 (Fig. 2(c)) are more gentle compared to the curves for organoclay CEC 50 (Fig. 2(b)). Moreover, the breakthrough points for organoclays appeared earlier than those of washed clay, and the

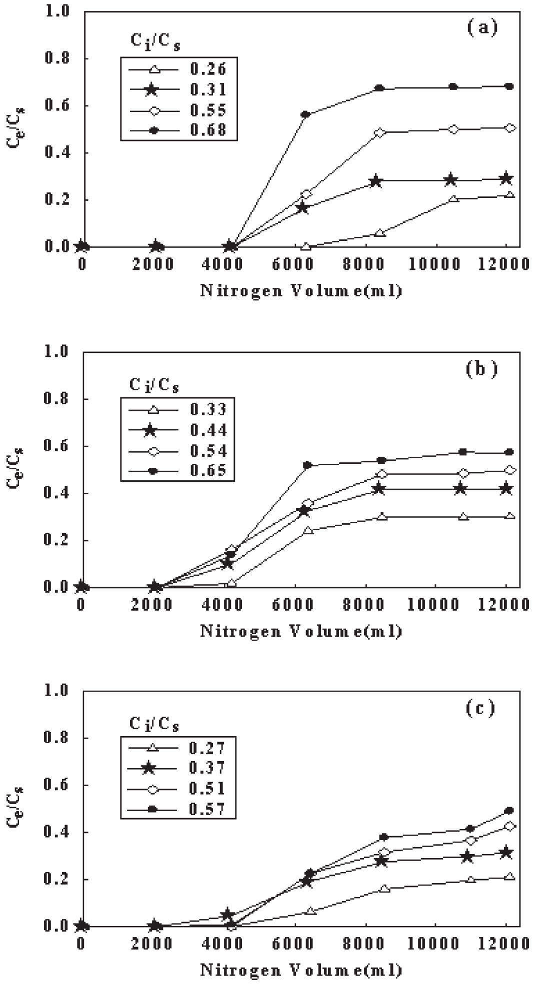

Figure 2. Adsorption breakthrough curves of chlorobenzene on washed clay (a), organoclay CEC 50 (b), and organoclay CEC 100 (c). The curves represent the effluent concentration responding to the various inlet concentration of chlorobenzene.

effluent concentrations increased slowly before they reach the final stabilizing concentrations. This trend became more apparent as the HDTMA loading of organoclay increased and as the inlet concentrations of VOC became greater. These results imply that as the HDTMA loading on the clay surface increases, the mass transfer zone becomes broader due to the increased mass transfer resistance at the interface of the gas phase and the clay. It has been recognized that as the concentration of surfactant increases on the clay surface, the hydrophobic tails of the surfactant molecules tend to associate to form multilayers on the clay surface. These phenomena may provide not

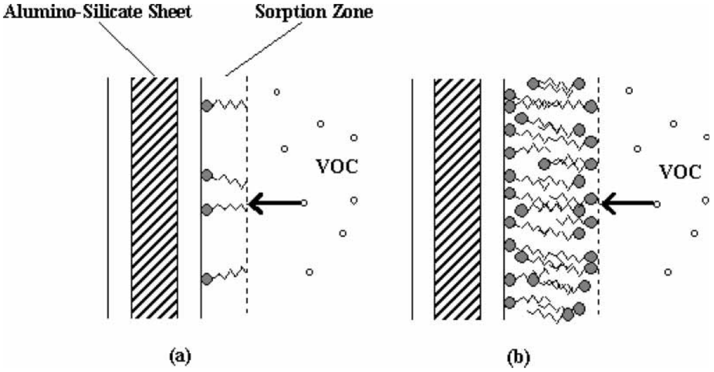

Figure 3. Schematic model that describes the adsorption surface of lower-surfactant-loading organoclay (a) and that of higher-surfactant-loading organoclay (b).

only the more adsorption sites for VOCs but also the higher mass transfer resistance for diffusing molecules from a gas to a clay surface.

Figure 3 illustrates a schematic model that describes the adsorption surface of lower-surfactant-loading organoclay (a) and that of higher-surfactant-loading organoclay (b). The figure shows the formation of the sorption zone at the interface of the clay surface (alumino-silicate sheet) and gas phase which is induced by the presence of surfactant molecules. In the washed clay, this sorption zone does not exist.

The thickness of this sorption zone may be proportional to the degree of surfactant loading, and the higher surfactant concentration may cause the formation of multilayers on the clay surface. The increase of adsorption capacity in organoclay CEC 100 is attributed to the enlarged sorption zone in which the molecules of VOCs can be captured.

Figure 4 shows the adsorption breakthrough curves of trichloroethylene on washed clay (a) and on organoclay CEC 100 (b). In case of adsorption experiments of trichloroethylene, only the low range of inlet concentration ($0.19-0.29C_s$) was used. In Fig. 4, the breakthrough points of trichloroethylene are located somewhere between the origin and a point on x-axis at which ca. 2000 ml of nitrogen was utilized. The saturated concentration of trichloroethylene in nitrogen was 93,000 ppm. It was found that in these low inlet concentration ranges, there was no significant difference in the breakthrough behavior for washed and organoclays.

Adsorption Isotherms

The breakthrough curves shown in Figs. 2 and 4 were analyzed by Eq. (1) to calculate the mass of adsorption, which was divided by the weight of clay in the bed to give the amount of uptake per unit mass of clay. Figure 5 shows the

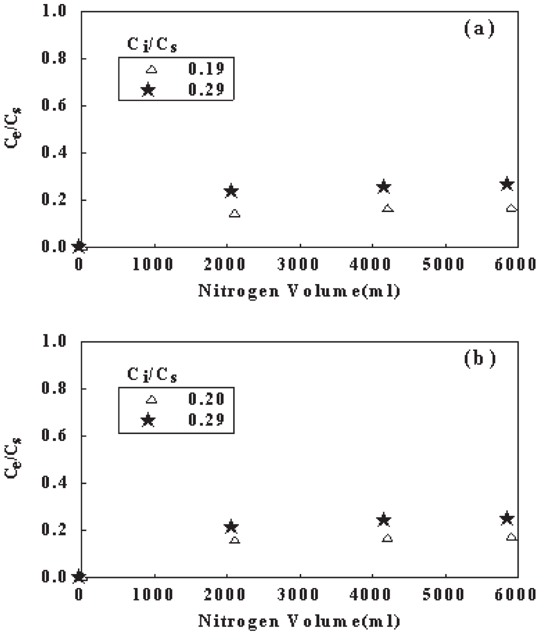

Figure 4. Adsorption breakthrough curves of trichloroethylene on washed clay (a) and organoclay CEC 100 (b). The curves represent the effluent concentration responding to the various inlet concentrations of trichloroethylene.

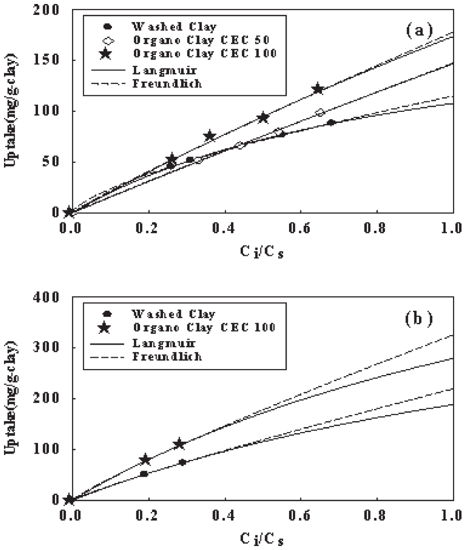

Figure 5. Langmuir and Freundlich adsorption isotherms of chlorobenzene (a) and trichloroethylene (b) on washed clay, organoclay CEC 50, and organoclay CEC 100.

uptake of chlorobenzene (a) and trichloroethylene (b) as a function of the inlet concentration of a VOC in nitrogen.

In Fig. 5, the experimental data were used to model two adsorption isotherm equations. First, the Langmuir isotherm equation was used as follows.

$$q_e = \frac{q_m bC}{1 + bC} \tag{2}$$

where q_e is the uptake of a VOC per unit mass of clay, q_m is the monolayer adsorption capacity, b is the adsorption equilibrium constant, and C is the equilibrium concentration of gas phase. In addition to the Langmuir isotherm, the Freundlich isotherm equation was used as follows.

$$q_e = kC^{1/n} \tag{3}$$

where k is the equilibrium constant and n is the empirical constant. We adopted the Langmuir and Freundlich isotherms because these equations are the most popularly used isotherms, and we intended to examine if the two isotherms could successfully fit the adsorption data. In addition these isotherms provide the information on the monolayer adsorption capacity and the equilibrium constant. The two adsorption isotherm equations were fitted using experimental data with correlation coefficients greater than 0.999 for all isotherms. The obtained constants for Eqs. (2) and (3) are listed in Table 3. It was found that the monolayer adsorption capacity q_m and the adsorption equilibrium constant b for Langmuir isotherm and the equilibrium constant k for Freundlich isotherm obviously increased with the HDTMA loading for both chlorobenzene and trichloroethylene.

The isotherms in Fig. 5 show that the adsorption capacity for chlorobenzene and trichloroethylene increased in the sequence of washed clay, organoclay CEC 50, and organoclay CEC 100. A minor exception was observed in the low concentration range of chlorobenzene (Fig. 5(a)), where the washed clay exhibited a slightly higher or an almost equal uptake compared to the organoclay CEC 50. These results imply that at a

Table 3. Adsorption isotherm constants for Langmuir and Freundlich isotherm equations

		Langmuir		Freundlich	
VOC	Clay	q_m (mg/g-clay)	b (L/mg)	k(L/g-clay)	n
CB	Washed	156.8	0.0642	115.3	1.458
	CEC 50	208.9	0.198	148.0	1.038
	CEC 100	221.8	1.049	178.6	1.092
	Washed	297.6	0.571	220.3	1.134
	CEC 100	449.9	0.605	326.7	1.146

low concentration range of VOCs, the adsorption capacity of the three types of clays may be similar. At a high concentration of VOCs, however, the organoclays showed an enhanced adsorption capacity compared to the washed clay, and the adsorption capacity increased with the HDTMA loading on clay surface. In Fig. 5, the adsorption isotherms extrapolated the experimental data and the resulting isotherms predicted the adsorption capacity that can be obtained when the inlet concentration of a gas stream is saturated with VOCs. It was found that the saturation capacity predicted by the Freundlich isotherm was slightly higher than the capacity predicted by the Langmuir isotherm. Based on the extrapolated value by the Langmuir isotherm, the adsorption capacity of organoclay CEC 100 exceeded that of washed clay by 60% for chlorobenzene and 55% for trichloroethylene, respectively.

Figure 5 shows that the saturation capacities of trichloroethylene are greater that those of chlorobenzene. This can be explained by the higher vapor pressure of trichloroethylene than chlorobenzene. Due to the higher vapor pressure of trichloroethylene, the saturation concentration C_s of trichloroethylene in nitrogen became much higher than that of chlorobenzene, which caused the larger saturation capacity of trichloroethylene compared to chlorobenzene.

Desorption Profiles and their Modeling

Desorption was conducted by flowing pure nitrogen through the adsorption bed immediately after a set of adsorption experiments was completed. Desorption data were obtained by measuring effluent concentrations as a function of time, and the data were plotted as a function of the nitrogen used. Figures 6 and 7 show the typical desorption profiles of chlorobenzene and trichloroethylene, respectively. Figure 6(a) shows the desorption profiles of chlorobenzene for washed clay and these data were obtained from desorption experiments of clays whose adsorption breakthrough curves were as shown in Fig. 2(a). Similarly, the data in Fig. 6(b) are the desorption profiles for organoclay CEC 100 and these data were obtained from clays whose adsorption curves were as shown in Fig. 2(c). The experimental data in Fig. 6(c) is identical to those in Fig. 6(b), but these two figures contain the curves that were calculated from two different models. Figure 7 shows the desorption profiles of trichloroethylene for washed clay (a), organoclay CEC 100 (b and c), respectively, and the Figs. 7(b) and 7(c) contain the curves that were calculated from two different models. Overall observation indicated that the desorption profiles monotonically decreased with time (or with the amount of nitrogen used).

The desorption profiles were analyzed by adopting two different models that had been applied for our previous research (14). Firstly, the system was simplified by assuming that the gas stream in the bed was efficiently mixed and the concentration gradient inside the bed was negligible. Therefore, the

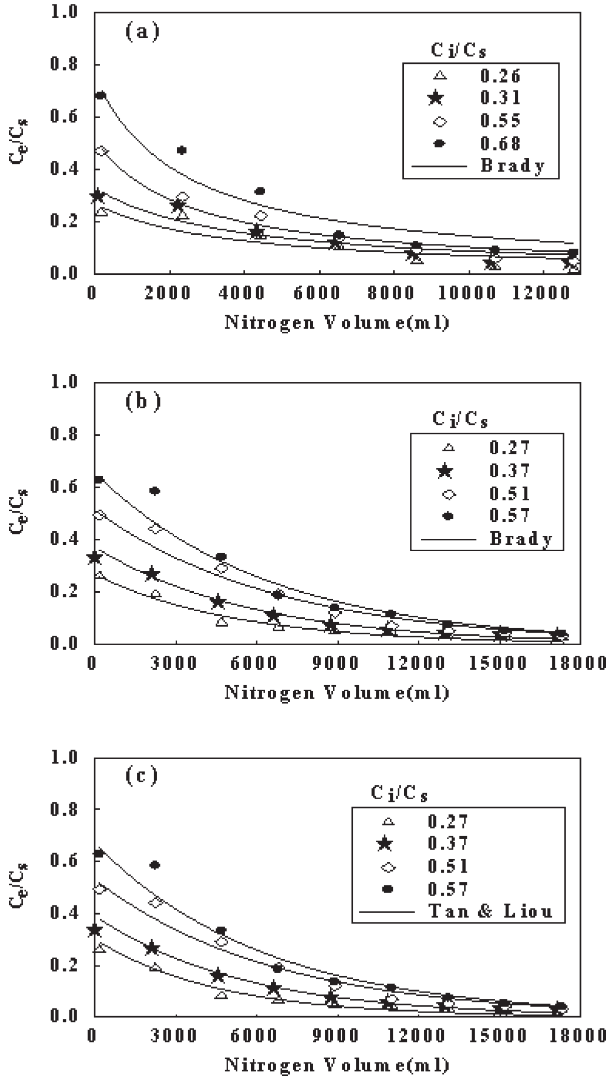

Figure 6. Desorption profiles of chlorobenzene from washed clay (a), organoclay CEC 100 with the Brady model (b), organoclay CEC 100 with the Tan & Liou model (c).

equilibrium was the only factor contributing to the desorption process. Based on this assumption, Brady et al. suggested the following mass balance equation over the desorption bed (15).

$$W\frac{d\theta}{dt} = -VC \tag{4}$$

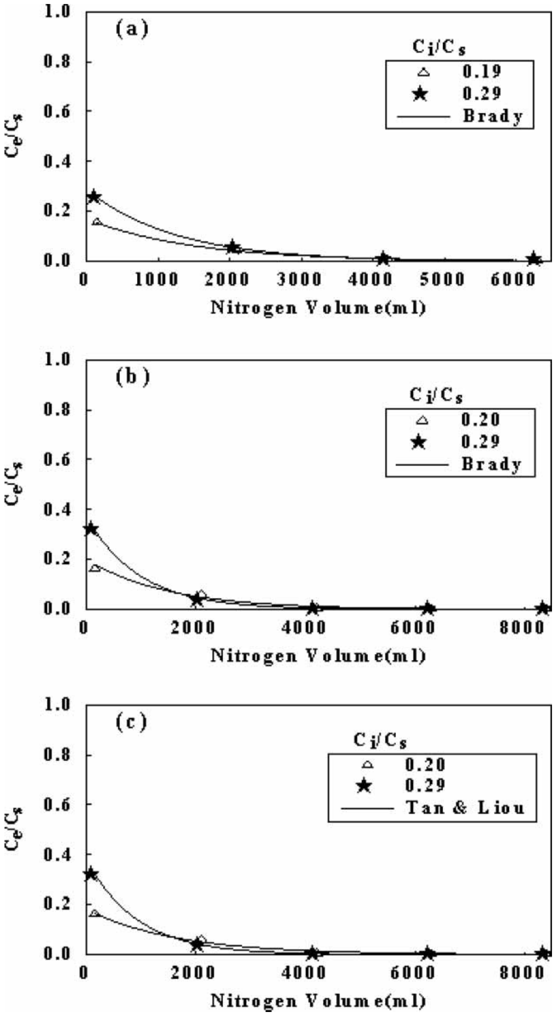

Figure 7. Desorption profiles of trichloroethylene from washed clay (a), organoclay CEC 100 with the Brady model (b), organoclay CEC 100 with the Tan & Liou model (c).

where W is the mass of clay, θ is the VOC concentration in the clay phase, V is the volume flow rate of the gas phase, and C is the VOC concentration in the gas phase. The VOC concentrations of the two phases are linearly related as follows.

$$\theta = KC \tag{5}$$

where K is the distribution coefficient of VOC between clay and gas phases. Using Eq. (5) the solution of Eq. (4) becomes,

$$\ln(\theta/\theta_0) = \left(-\frac{V}{KW}\right)t \tag{6}$$

where θ_o is the initial VOC concentration in the clay phase. Eq. (6) allows the calculation of the distribution coefficient K by fitting the experimental data with the desorption profiles. This simplified linear model might be inaccurate for modeling a fixed bed. However, the adsorption bed used in this study was of relatively short length and the flow rate of the gas phase relatively low, hence equilibrium could be attained in the adsorption bed.

Secondly, we adopted another model that was suggested by Tan and Liou (16). A material balance in the bed (without considering the axial dispersion) can be written as

$$\varepsilon\frac{\partial C}{\partial t} + u\frac{\partial C}{\partial z} = -(1-\varepsilon)\frac{\partial S}{\partial t} \tag{7}$$

where ε is the bed porosity, u is the superficial velocity of gas stream, and S is the VOC concentration per unit volume of clay. The initial and boundary conditions are at $t = 0$, $C = 0$ and $z = 0$, $C = 0$. The linear desorption kinetics used is as follows.

$$\frac{\partial S}{\partial t} = -kS \tag{8}$$

where k is the desorption rate constant. The initial condition is at $t = 0$, $S = S_o$. The solution of Eqs. (7) and (8) with the initial and boundary conditions gives the expression for the concentration at the exit of adsorption bed C_e.

$$C_e = \frac{1-\varepsilon}{\varepsilon}S_0\left\{\exp\left[-k\left(t-\frac{\varepsilon L}{u}\right)\right] - \exp(-kt)\right\} \tag{9}$$

where L is the bed length. The amount of desorption can be calculated by integrating C_e with respect to time. The desorption rate constant k is determined by the regression of Eq. (9) with the experimental data.

The desorption profiles that were calculated from two models (Brady and Tan & Liou models) are shown in Figs. 6 and 7. The two models successfully fit the desorption data by adjusting two parameters (the distribution coefficient K for the Brady model and the desorption rate constant k for the Tan & Liou model). The evaluated values of the distribution coefficient K and the desorption rate constant k are listed in Table 4. In this table, C_i/C_s stands for the inlet concentration of the gas stream when the clay was used for adsorption experiments. It was found that the evaluated distribution coefficients and desorption rate constants of a particular VOC did not show any significant difference for a given type of clay. The values were almost constant regardless of the inlet concentration and the type of clay. The distribution coefficient and desorption rate

Table 4. Distribution coefficient *K* and desorption rate constant *k* used for desorption profiles

VOC	Clay	C_i/C_s	$K(\mathrm{cm}^3/\mathrm{g})$	$k\ (\mathrm{min}^{-1})$
CB	Washed	0.26	2514.2	0.000156
		0.31	2269.4	0.000175
		0.55	2107.1	0.000187
		0.68	1958.6	0.000202
	CEC 50	0.33	1463.8	0.000265
		0.44	2033.3	0.000231
		0.54	1770.2	0.000219
		0.65	1812.0	0.000214
	CEC 100	0.27	2030.4	0.000194
		0.37	2253.8	0.000172
		0.51	2647.5	0.000166
		0.57	2502.3	0.000154
TCE	Washed	0.19	580.6	0.000629
		0.29	483.7	0.000715
	CEC 100	0.20	581.5	0.000600
		0.29	376.3	0.001091

constant of chlorobenzene were in the range of 1770.2–2647.5 cm^3/g and 0.000154–0.000265 min^{-1}, respectively, for all types of clays and for all ranges of VOC concentrations. The distribution coefficient and desorption rate constant of trichloroethylene were in the range of 376.3–581.5 cm^3/g and 0.0006–0.001 min^{-1}, respectively. The distribution coefficient *K* of chlorobenzene was an order of magnitude greater than that of trichloroethylene, and the desorption rate constant of trichloroethylene was much higher than that of chlorobenzene. These results indicated that trichloroethylene was more likely to transfer from clay to a gas phase compared to chlorobenzene, and therefore it was easier to remove trichloroethylene from clays than chlorobenzene.

In our previous study (14), we have found that the adsorption capacity of organoclays was not damaged during the repeated processes of adsorption and desorption experiments. Therefore, the organoclays that processed by desorption experiment can be recycled for further adsorption of VOCs. In this respect, the present study shows the potential capability of organoclays for adsorption media of gaseous organic contaminants and demonstrates the possible regeneration method of used organoclays using vapor extraction technology.

CONCLUSIONS

Adsorption and desorption of chlorobenzene and trichloroethylene were carried out using washed clay, organoclay CEC 50, and organoclay

CEC 100. The shape of the breakthrough curves indicated that as the HDTMA loading on the clay surface increased, the mass transfer zone became broader due to the higher mass transfer resistance at the interface of the gas and the clay surface. Adsorption data were well represented by Langmuir and Freundlich isotherms. Organoclays showed the higher adsorption capacity compared to washed clay, and the adsorption capacity increased with the amount of the HDTMA loading on the organoclay. Desorption profiles were fitted by two different models, and the distribution coefficients and desorption rate constants were evaluated. The results revealed that trichloroethylene was easier to be desorbed from clays compared to chlorobenzene.

REFERENCES

1. Xi, Y.F., Frost, R.L., and He, H.P. (2007) Modification of the surfaces of Wyoming montmorillonite by the cationic surfactants alkyl trimethyl, dialkyl dimethyl, and trialkyl methyl ammonium bromides. *J. Colloid Interf. Sci.*, 305: 150.
2. Oyanedell-Craver, V.A. and Smith, J.A. (2006) Effect of quaternary ammonium cation loading and pH on heavy metal sorption to Ca bentonite and two organobentonites. *J. Hazard. Mater.*, 137: 1102.
3. Wiles, M.C., Huebner, H.J., Mcdonald, T.J., Donnelly, K.C., and Phillips, T.D. (2005) Matrix-immobilized organoclay for the sorption of polycyclic aromatic hydrocarbons and pentachlorophenol from groundwater. *Chemosphere*, 59: 1455.
4. Boyd, S.A., Shaobai, S., Lee, J.F., and Mortland, M.M. (1998) Pentachlorophenol sorption by organo-clays. *Clays Clay Miner.*, 36: 125.
5. Tian, S.L., Zhu, L.Z., and Shi, Y. (2004) Characterization of sorption mechanisms of VOCs with organobentonites using a LSER approach. *Environ. Sci. Technol.*, 38: 489.
6. Carrizosa, M.J., Rice, P.J., Koskinen, W.C., Carrizosa, I., and Hermosin, M.D. (2004) Sorption of isoxaflutole and DKN on organoclays. *Clays Clay Miner.*, 52: 341.
7. He, H.P., Zhou, Q., Martens, W.N., Kloprogge, T.J., Yuan, P., Yunfer, X.F., Zhui, J.X., and Frost, R.L. (2006) Microstructure of HDTMA(+)-mofified montmorillonite and its influence on sorption characteristics. *Clays Clay Miner.*, 54: 689.
8. Nzengung, V.A., Voudrias, E.A., Nkedi-Kizza, P., Wampler, J.M., and Weaver, C.E. (1996) Organic cosolvent effects on sorption equilibrium of hydrophobic organic chemicals by organoclays. *Environ. Sci. Technol.*, 30: 89.
9. Zhang, Z.Z., Sparks, D.L., and Scrivner, N.C. (1993) Sorption and desorption of quaternary amine cations on clays. *Environ. Sci. Technol.*, 27: 1625.
10. Dentel, S.K., Bottero, J.Y., Khatib, K., Demougeot, H., Duguet, J.P., and Anselme, C. (1995) Sorption of tannic acid, phenol, and 2,4,5-trichlorophenol on organoclays. *Wat. Res.*, 29: 1273.
11. Haggerty, G.M. and Bowman, R.S. (1994) Sorption of chromate and other inorganic anions by organo-zeolite. *Environ. Sci. Technol.*, 26: 452.
12. Yeo, S.D., Tuncer, E., and Akgerman, A. (1997) Adsorption of volatile organic compounds on soil and prediction of desorption breakthroughs. *Sep. Sci. Technol.*, 32: 2497.

13. McCabe, W.L., Smith, J.C., and Harriott, P. (2005) *Unit Operations of Chemical Engineering*, 7th Edn.; McGraw-Hill Co.: New York.
14. Park, S.J. and Yeo, S.D. (1999) Supercritical extraction of phenols from organically modified smectite. *Sep. Sci. Technol.*, 34: 101.
15. Brady, B.O., Kao, C.P.C., Dooley, K.M., Knopf, F.C., and BGambrell, R.P. (1987) Supercritical extraction of toxic organics from soils. *Ind. Eng. Chem. Res.*, 26: 261.
16. Tan, C.S. and Liou, D.C. (1988) Desorption of ethyl acetate from activated carbon by supercritical carbon dioxide. *Ind. Eng. Chem. Res.*, 27: 988.